

Diblock Copolymer Formation via Self-Assembly of Cyclodextrin and Adamantyl End-Functionalized Polymers

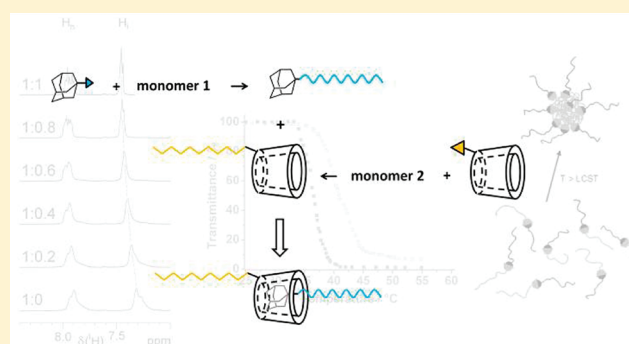
Jan Stadermann,[†] Hartmut Komber,[†] Michael Erber,[†] Frank Däbritz,[†] Helmut Ritter,[‡] and Brigitte Voit^{†,*}

[†]Leibniz Institut fuer Polymerforschung Dresden e.V., Hohe Strasse 6, 01069 Dresden, Germany

[‡]Lehrstuhl für Präparative Polymerchemie, Institut für Organische Chemie und Makromolekulare Chemie, Heinrich-Heine Universität, Universitätsstrasse 1, Geb. 26.33.00, D-40225 Düsseldorf, Germany

S Supporting Information

ABSTRACT: Two water-soluble polymers poly(2-methyl-2-oxazoline) and poly(*N*-isopropylacrylamide) with complexing moieties (β -CD and adamantane, respectively) located at the chain ends were prepared via controlled techniques. To verify the interaction of the β -CD- and adamantane-type polymer end groups in aqueous solution, detailed complexation studies were carried out by ¹H NMR spectroscopy. It could be proved, that the polymers undergo self-assembly to form the corresponding supramolecular diblock structure. Furthermore, the double-hydrophilic block assembly was observed to be switchable to a hydrophilic–hydrophobic configuration by adjusting temperature leading to reversible aggregate formation.



INTRODUCTION

Cyclodextrins (CDs) are of particular interest in polymer chemistry, e.g., for CD-mediated polymerizations.¹ Further, CDs have been used as building blocks for the construction of polymeric networks. These gels are chemically cross-linked materials where CD is covalently incorporated^{2,3} or physical assemblies formed through noncovalent interactions of the CD units.⁴ Various CD-containing structures have been designed and studied, e.g., in view of pharmaceutical applications like drug carrier systems.^{5–7}

By using the complexation of CDs with nonpolar moieties of appropriate size, the design of reversible polymer networks is possible. Those can be broken by addition of competitive low-molecular molecules or by increasing temperature.⁸ In particular, the high binding forces in host–guest inclusion complexes between β -CD and adamantyl groups have often been exploited in building up supramolecular assemblies.^{9–11} Resulting reversible gel systems are considered to be interesting, e.g., as injectable drug delivery depots.

With respect to an increasing demand for more defined polymer structures, there is a high interest in a controlled design of CD-mediated assemblies by taking advantage of the highly specific click chemistry. By using azide-functionalized CD, it is possible to selectively equip alkyne-functionalized polymer materials or surfaces with CD-moieties.^{12,13} On the other hand, novel CD-functionalized monomers are accessible via the “click-strategy”. The group of Ritter reported the synthesis of monofunctionalized β -CD-functionalized acrylate and methacrylate¹⁴ as well as *N*-vinylpyrrolidone¹⁵ via the click reaction. By copolymerization with

N-isopropylacrylamide (NIPAAm)¹⁴ and with *N*-vinylpyrrolidone,¹⁵ respectively, copolymers were obtained with up to 10 mol % comonomer bearing covalently attached β -CD as backbone functionality. Further, Nielsen et al. reported the synthesis of β -CD-dextran polymers from alkyne-modified dextrans using the click-approach.¹⁶ These polymers were studied with respect to their binding properties to adamantane derivatives.^{14–16}

In general, different types of noncovalent interactions can be exploited for the construction of reversible supramolecular architectures.^{17,18} Cordier et al. reported the design of reversible networks, being rubber-like materials which show self-healing behavior, where the assembly is formed via functional units able to associate through multiple hydrogen bonds.¹⁹ The use of strong hydrogen bonds is also described for the assembly of linear polymer chains,²⁰ diblock copolymers²¹ and other block structures.²² Further, the design of diblock and triblock polymer structures via directed metal coordination was demonstrated by the group of Schubert.^{23–25}

However, reports which address the assembly of polymeric structures through CD-adamantane complexation are so far limited to reversible gel systems. In contrast, this work is concerned with the building up of defined diblock copolymers via complexation of β -CD and adamantane as polymer end group functionalities. Herein, this concept is demonstrated with two water-soluble polymers: poly(2-methyl-2-oxazoline) (PMeOxa)

Received: January 12, 2011

Revised: March 24, 2011

Published: April 08, 2011

and poly(*N*-isopropyl-acrylamide) (PNIPAAm), both being of high interest for use in physiological systems. We present a versatile synthetic way to prepare defined end-functional polymers able to undergo self-assembly through the formation of strong inclusion complexes. Furthermore, studies on the β -CD-adamantane end group interaction are demonstrated yielding a well-defined diblock assembly.

The combination of PNIPAAm and PMeOxa in such a self-assembled diblock can be described as a double-hydrophilic system. However, due to the well-known thermoresponsive character of PNIPAAm, this diblock structure is switchable to a hydrophilic–hydrophobic configuration as a consequence of the heat-induced PNIPAAm phase transition at a lower critical solution temperature (LCST). The hydrophilic part is realized by PMeOxa which does not show a thermoresponsive behavior in this temperature range. Such a switching process strongly influences the aggregation behavior, which is hence controllable by adjusting temperature.²⁶ Consequently, these materials are highly interesting, if the change in aggregation can be related to a controlled drug release.^{27,28} On the other hand, the supramolecular polymer coupling is controllable by means of temperature owing to the enthalpic nature of the β -CD-adamantane inclusion complex.²⁹

Various block and graft copolymers composed of PNIPAAm and PMeOxa have been prepared via conventional methods so far.^{30,31} Here we present the synthesis of an adamantane-containing initiator for the cationic ring-opening polymerization and a β -CD-containing initiator for the atom transfer radical polymerization (ATRP). These functional initiators are then employed to initiate the polymerization of 2-methyl-2-oxazoline and *N*-isopropylacrylamide, respectively. NMR studies finally prove the successful complex formation of the head-functionalized polymers leading to noncovalent diblock assembly. Furthermore, the influence of the thermoresponsive behavior of the PNIPAAm block on the complex stability is studied.

EXPERIMENTAL SECTION

Methods. GPC measurements were performed on a Polymer Laboratories PL-GPC 50 Plus Integrated GPC System equipped with a microvolume double piston pump of Agilent Technologies. *N,N*-Dimethylacetamide (DMAc) containing 3 g/L LiCl was used as eluent at a flow rate of 1.0 mL/min. A PolarGel-M column of Polymer Laboratories connected to a Mini DAWN light scattering (LS) detector of Wyatt Technology was applied. All polymers were dissolved in DMAc and filtered through a 0.2 μ m PTFE filter. Data were processed with ASTRA software.

NMR spectra were recorded on a Bruker Avance III 500 NMR spectrometer operating at 500.13 MHz for ¹H and at 125.75 MHz for ¹³C using a 5 mm quad (¹H, ¹³C, ¹⁹F, ³¹P) inverse probe, equipped with a shielded z-gradient coil. The solvent signals were used as internal standard: DMSO-*d*₆: δ (¹H) = 2.50 ppm, δ (¹³C) = 39.6 ppm and CDCl₃: δ (¹H) = 7.26 ppm, δ (¹³C) = 77.0 ppm, respectively. Spectra recorded from D₂O solutions were referenced on external sodium 3-(trimethylsilyl)propionate-2,2,3,3-*d*₄ (δ (¹H) = 0 ppm). These spectra were recorded applying a spectral width of 6000 Hz digitized into 64K points and a recycle time of 10 s. The concentration of both components in the complexation experiments was 5×10^{-3} M for the 1:1 complex. However, due to titration of one component by the second one the concentrations are different at different degree of complexation. For the temperature-dependent experiments and for the 2D ROESY experiments also 5×10^{-3} M solutions of the 1:1 complex were used. For temperature-dependent ¹H NMR measurements, the temperature was

controlled by the Bruker variable temperature accessory BVT-3000 and was calibrated using the standard Wilmad ethylene glycol sample. In all measurements the temperature was maintained constant within ± 0.2 K. After each temperature step ($\Delta T = 4$ K) the sample was allowed to equilibrate for 15 min. The 2D ROESY spectrum was recorded with cw spinlock using a loop of 690 ($180^\circ_x - 180^\circ_{-x}$) pulses of 180 μ s length of the 180° pulse giving a total mixing time of 248 ms (phase sensitive using TPPI, 24 scans, sweep width = 4746 Hz, 2K data points in F2 and 256 experiments in F1). Further standard 2D NMR spectra were recorded to verify the ¹H and ¹³C signal assignments for initiators and polymers using standard parameters.

DSC analysis were performed with a differential scanning calorimeter Q1000 of TA Instruments (USA) in nitrogen atmosphere from -80 °C to $+200$ °C at a scan rate of 10 K/min. *T*_g values were determined using the half-step method.

Mass spectra were acquired on a Biflex II MALDI-TOF MS system (Bruker Daltonics, Germany). The measurements were carried out in reflector mode and positive polarity using an ion acceleration voltage of 20 kV.

Dynamic light scattering (DLS) measurements were performed using a Zetasizer NanoZS Instrument (MALVERN Instruments, Worcestershire, UK) equipped with a 4 mW He–Ne-laser ($\lambda = 633$ nm) and with noninvasive backscattering (NIBS) detection at a scattering angle of 173°. The solutions were prepared in ultrapure water and filtered using a 0.20 μ m disposable PTFE filter.

The cloud point temperature of the polymer solutions was measured with a Specord M40 UV/vis spectrometer from Analytik Jena (Germany). The spectrometer is equipped with a Peltier cell holder for temperature control. The turbidity of the solutions was monitored as a function of temperature at a specific wavelength λ of 400 nm and under continuous stirring. Solutions were prepared in a concentration of 2 mg/mL using distilled water.

Materials. The azide-functionalized β -cyclodextrin (β -CD) mono-(6-azido-6-desoxy)- β -cyclodextrin was synthesized according to the literature¹⁵ and monofunctionalization was proven (details on synthesis and characterization see Supporting Information). 2-Methyl-2-oxazoline (Aldrich, 98%) was purified by distillation over calcium hydride (CaH₂). 2-(Isopropylamino)ethanol (Aldrich, 70%) was purified by distillation. The following chemicals were purchased from Aldrich and used as received (purity level): 2-bromoisobutyl bromide (98%), 3-(trimethylsilyl)propargyl alcohol (99%), tetrabutylammonium fluoride solution (1.0 M in THF), 1-adamantanemethanol (99%), *p*-bromomethylbenzoyl bromide (96%), triethylamine (99.5%), *N,N*-diisopropylethyl amine (99%), copper(I) iodide (99.5%), copper(I) bromide (99.999%), *N*-isopropylacrylamide (NIPAAm) (99%), and tris[2-(dimethylamino)ethyl]amine (Me₆TREN). All solvents were purchased from Aldrich and used without further purification.

Synthesis. 2-Bromoisobutyl Propargylester (**A**). The alkyne **A** was synthesized according to the given description (see Supporting Information).

Initiator I-1. **I-1** was synthesized according to the literature.³² Using argon as protection gas, 1-adamantanemethanol (1 g, 6.02 mmol) was dissolved in dichloromethane (30 mL) and dry Et₃N (0.61 g, 6.01 mmol). After cooling to 0 °C, *p*-bromomethylbenzoyl bromide (2.39 g, 8.60 mmol) was added step by step. Afterward, the solution was stirred under reflux for 1 h. The solvent and residual Et₃N was removed under vacuum and the crude product was purified by means of column chromatography using silica gel with hexane/dichloromethane as eluent (gradient: 10–30% dichloromethane) yielding **I-1** as a colorless solid. Yield: 1.77 g (81%). Mp: 75 °C.

¹H NMR (CDCl₃): δ (ppm) = 8.03 (d, 2H, H_b), 7.46 (d, 2H, H_i), 4.50 (s, 2H, H_l), 3.93 (s, 2H, H_e), 2.02 (m, 3H, H_b), 1.77 and 1.70 (AB spin system, ²J_{HH} = 12.1 Hz, 6H, H_a), 1.64 (d, ³J_{HH} = 2.4 Hz, 6H, H_c). ¹³C NMR (CDCl₃): δ (ppm) = 166.08 (C_i), 142.50 (C_k), 130.60 (C_g),

130.05 (C_h), 129.01 (C_i), 74.37 (C_e), 39.45 (C_c), 37.00 (C_a), 33.56 (C_d), 32.25 (C_f), 28.09 (C_b).

Anal. Calcd for C₁₉H₂₃BrO₂: C, 62.82; H, 6.38. Found: C, 62.87; H, 6.51.

Initiator I-2. 2-Bromoisobutyryl propargyl ester (0.1 g, 0.49 mmol) and copper(I) iodide (20 mg, 0.11 mmol) were added under nitrogen atmosphere to a solution of mono(6-azido-6-desoxy)- β -cyclodextrin (0.3 g, 0.26 mmol) (ratio alkyne/azide = 1.9: 1) in 30 mL DMF. Afterward, diisopropylethyl amine (0.13 g, 1.0 mmol) was added and the solution was allowed to stir under nitrogen atmosphere for 14 h at room temperature. For working up, the mixture was poured into 200 mL of toluene. Next, about 100 mL of *n*-hexane were added, leading to precipitation of the product. The yellowish solid was isolated by filtration and washed several times with diethyl ether. Yield: 310 mg (87%). Mp: 227 °C.

¹H NMR (DMSO-*d*₆): δ (ppm) = 8.12 (s, 1H, H₇), 5.9–5.6 (14H, CH–OH), 5.23 (s, 2H, H₉), 5.03 and 4.9–4.7 (7H, H_{1,1'}), 4.88 and 4.60 (m, 2H, H_{6'}), 4.55–4.2 (6H, CH₂–OH), 4.00 (t, 1H, H_{5'}), 3.8–3.5 (23H, H_{3,5,6,3'}), 3.4–3.2 (H_{2,4,2',4'}; overlaps with DHO), 3.08 and 2.89 (m, 2H, H₆ of the glucose unit bonded to C_{1'}),¹⁶ 1.88 (s, 6H, H₁₂). ¹³C NMR (DMSO-*d*₆): δ (ppm) = 170.44 (C₁₀), 141.35 (C₈), 125.67 (C₇), 102.5–101.5 (C₁), 101.24 (C_{1'}), 83.35 (C_{4'}), 82.0–81.0 (C₄), 73.5–71.5 (C_{2,3,5,2',3'}), 69.87 (C_{5'}), 60.5–59.5 (C₆), 58.96 (C₆ of the glucose unit bonded to C_{1'}), 58.77 (C₉), 56.94 (C₁₁), 50.35 (C_{6'}), 30.16 (C₁₂).

Ada-PMeOxa (P-1). The adamantyl-containing initiator (I-1) (0.10 g, 0.28 mmol) was dissolved in dry benzonitrile (4.3 mL) under argon atmosphere. Next, dried 2-methyl-2-oxazoline (1.17 g, 13.76 mmol) was added. The solution was heated to 100 °C and stirred for 1.5 h. For determining the monomer conversion, a sample was taken and diluted with deuterated chloroform for NMR measurement. Without cooling the solution, 2-(isopropylamino)ethanol (0.28 g, 2.75 mmol) was added all at once for chain termination. The solution was stirred for further 10 min at 100 °C. After cooling to room temperature, the solution was diluted with dichloromethane and precipitated twice in diethyl ether (400 mL). The product was separated and dried under vacuum at 40 °C for 16 h. For subsequent dialysis, the solid was dissolved in water (12 mL) and a small amount of acetone was added until the solution became clear. After dialysis against water (800 mL) with cellulose membranes of MWCO1000, freeze-drying and subsequent drying under vacuum at 40 °C for 2 days, polymer P-1 was obtained as a yellow solid. Yield: 957 mg (74%).

¹H NMR (CDCl₃): δ (ppm) = 8.1–7.9 (H_n), 7.4–7.2 (H_i), 4.7–4.55 (H_l), 3.90 (H_e), 3.6–3.3 (H_{g,s}), 2.92 (H_p), 2.61 (H_r), 2.25–2.05 (H_n), 2.00 (H_b), 1.75 and 1.67 (AB spin system, H_a), 1.62 (H_c), 1.02 (H_q). ¹³C NMR (CDCl₃): δ (ppm) = 172–170 (C_m), 166.1 (C_f), 130.5–129.5 (C_{g,h}), 126.3 (C_i), 74.5 (C_e), 53–48.5 (C_l), 48.5–43 (C_o), 39.41 (C_c), 36.94 (C_a), 33.51 (C_d), 28.03 (C_b), 21.1 (C_n), 18.2 (C_q). Signals of C_k, C_v, and C_p could not be identified.

β -CD-PNIPAAm (P-2). In a 10 mL Schlenk flask, β -CD containing initiator I-2 (0.1 g, 0.074 mmol), NIPAAm (0.282 g, 2.5 mmol) and Me₆TREN (0.017 mL, 0.074 mmol) were dissolved in a mixture of 1.0 mL of water (Millipore) and 1.9 mL of DMF. The solution was degassed by means of four consecutive “freeze-pump-thaw cycles”. Next, CuBr (7.3 mg, 0.0051 mmol) as catalyst was added to the mixture. After one further “freeze-pump-thaw cycle”, the mixture was allowed to thaw in order to start the room temperature ATRP. After 1 h, the polymerization was quenched by abrupt freezing with liquid nitrogen followed by several drops of THF. The mixture was thawed and the solvent was removed under reduced pressure. For purification, the crude product was dissolved in 30 mL water which was slowly heated above the lower critical solution temperature. The precipitated polymer was separated and dried in vacuum at 50 °C to yield a colorless polymer. Yield: 172 mg (45%).

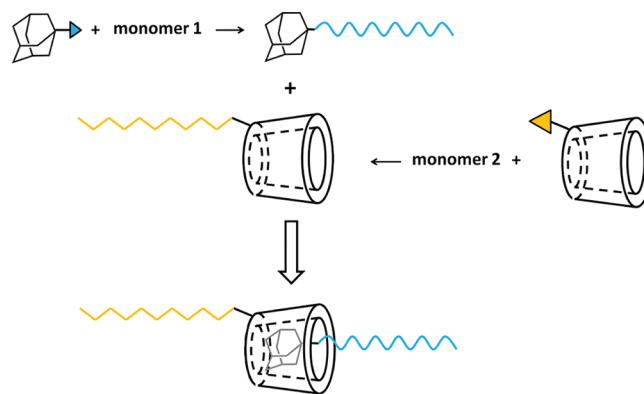


Figure 1. Synthetic strategy for noncovalent diblock formation via β -CD-adamantane complexation.

¹H NMR (DMSO-*d*₆): δ (ppm) = 8.02 (H₇), 7.5–6.9 (H_{1,6}), 5.9–5.6 (CH–OH), 5.05 (H₉), 5.03 and 4.9–4.75 (H_{1,1'}), 4.85 and 4.62 (H_{6'}), 4.55–4.2 (CH₂–OH), 3.98 (H_{5'}), 3.95–3.75 (H₁₇), 3.75–3.5 (H_{3,5,6,3'}), 3.5–3.2 (H_{2,4,2',4'}; overlaps with DHO), 3.13 and 2.94 H₆ of the glucose unit bonded to C_{1'}, 2.2–1.8 (H₁₄), 1.7–1.2 (H₁₃), 1.05 (H₁₈). ¹³C NMR: (DMSO-*d*₆) δ (ppm) = 173.4 (C₁₅), 141.9 (C₈), 125.7 (C₇), 102.5–102 (C₁), 101.5 (C_{1'}), 83.4 (C_{4'}), 82–81 (C₄), 73.5–71.5 (C_{2,3,5,2',3'}), 69.9 (C_{5'}), 61.5–59.0 (C₆), 57.2 (C₉), 50.3 (C_{6'}), 43–41 (C₁₄), 41.5–41 (C₁₇), 38–33 (C₁₃), 24–22 (C₁₈).

Self-Assembled Ada-PMeOxa/ β -CD-PNIPAAm (sa P-1/P-2). In a NMR tube, β -CD-PNIPAAm (P-2, 5.2 mg) was dissolved in D₂O (0.7 mL). Next, a D₂O solution (4.8 mg/mL) of Ada-PMeOxa (P-1) was added in portions until complete complexation was achieved as confirmed by NMR spectroscopy. Because of weighing errors for small amounts of substance and the inaccuracy of the M_n values, this is a proper approach to prepare the 1:1 complex. Subsequently, the solvent was removed under vacuum to yield sa P-1/P-2 as a white solid.

RESULTS AND DISCUSSION

Polymer Synthesis. Our approach toward the target PNIPAAm-PMeOxa diblock copolymers through self-assembly (sa) includes the synthesis of initiators bearing the units for complexation (β -cyclodextrin and adamantane, respectively) followed by polymerization via controlled methods. Mixing the obtained polymers in water is expected to give the respective diblock structure via self-assembly (Figure 1).

Figure 2 displays the reaction sequence for the preparation of the adamantane-functionalized poly(2-methyl-2-oxazoline) (Ada-PMeOxa, P-1). Initiator I-1 was obtained via esterification of 4-bromomethylbenzoyl bromide with 1-adamantanemethanol. The cationic polymerization of 2-methyl-2-oxazoline with I-1 was conducted at 100 °C for about 2 h and then stopped with the capper molecule 2-(isopropylamino)ethanol.

Figure 3 shows the ¹H NMR spectra of initiator I-1 and polymer P-1 recorded in DMSO-*d*₆. Both structures could be clearly confirmed via signal assignments. The characteristic signals of initiator I-1 are identified again in the polymer spectrum. While the signal of the benzyl protons of I-1 (signal l in Figure 3a) appears as a singlet, it changes to a multiplet in the polymer spectrum (signal l in Figure 3b) because of hindered rotation of the adjacent N–C bond due to amide mesomerism resulting in a varying chemical environment at position l. The characteristic adamantane signals (a–c) appear unchanged at

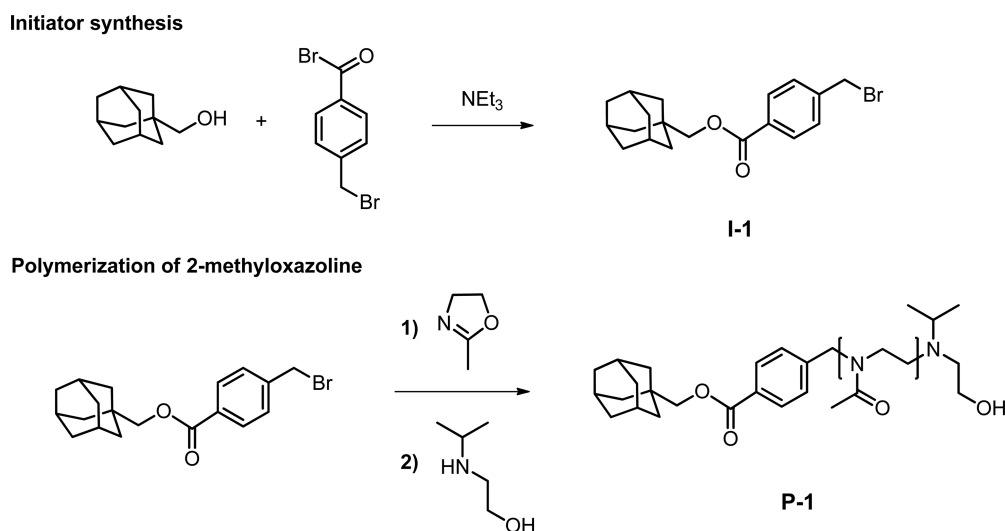


Figure 2. Reaction sequence for the synthesis of the adamantane-functionalized poly(2-methyl-2-oxazoline) (**P-1**).

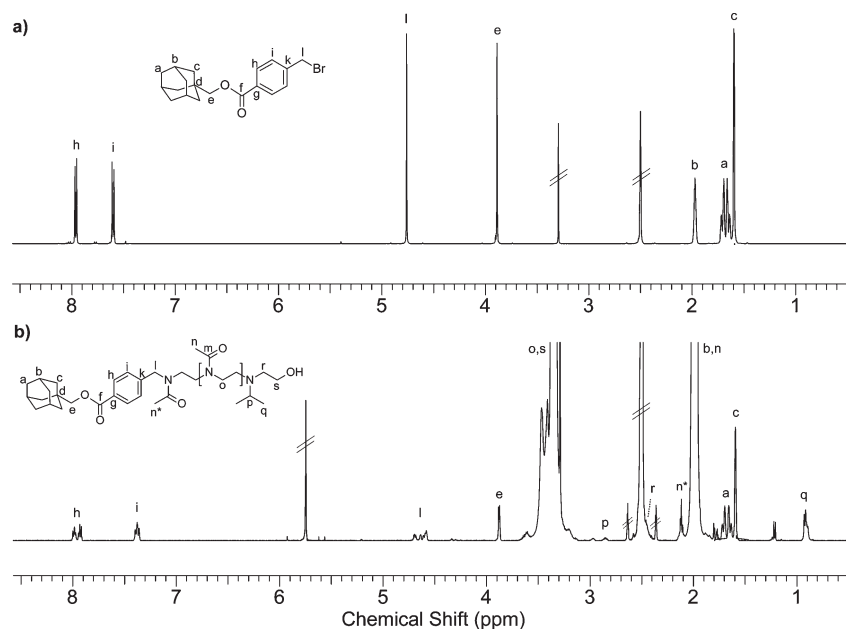


Figure 3. ^1H NMR spectra of initiator **I-1** (a) and polymer **P-1** (b) recorded in $\text{DMSO}-d_6$.

1.5–2.0 ppm. **P-1** was further studied by MALDI-TOF mass spectrometry (see Supporting Information).

The reaction sequence for the synthesis of the β -CD-functionalized poly(*N*-isopropylacrylamide) (β -CD-PNIPAAm, **P-2**) is shown in Figure 4. Starting with the monoazide-functionalized β -cyclodextrin (CD-N_3) (see ref 15 and Supporting Information) for synthesis and characterization), the ATRP-initiating moiety is introduced via the click reaction with 2-bromoisobutryl propargylester (**A**) (ratio alkyne/azide = 1.9:1). Next, the CD-functionalized initiator (**I-2**) was employed for initiation of the ATRP of NIPAAm to yield polymer **P-2**.

The click reaction with the alkyne **A** resulted in a quantitative functionalization of CD-N_3 , as confirmed by high yield of the product and the fully assigned ^1H NMR spectrum (efficient triazole ring formation seen e.g. by appearance of signal 7 and shift of signals 6' and 9, Figure 5a). Having the CD-functionalized

initiator (**I-2**) in hand allows for the synthesis of well-defined CD-initiated polymers of all monomers polymerizable via ATRP. In this work, initiator **I-2** was employed to start the polymerization of NIPAAm. The catalyst system $\text{CuBr}/\text{Me}_6\text{TREN}$ was used, which allows for room temperature ATRP. In the ^1H NMR spectrum of **P-2** (Figure 5b), the characteristic β -CD-signals of the initiator **I-2** are clearly identified.

The GPC chromatograms of the polymers **P-1** and **P-2**, obtained with a light scattering detector, are shown in Figure 6. The curves show narrow molar mass distributions, indicating a high degree of control of the corresponding polymerizations. In Table 1, synthesis data and characteristics of both polymers **P-1** and **P-2** are summarized.

For **P-1**, the molar mass calculated from the ^1H NMR spectrum (4200 g/mol), the one obtained by GPC using LS-detection (4600 g/mol) and the theoretical molar mass ($M_{n,\text{th}} = 4300$ g/mol) agree

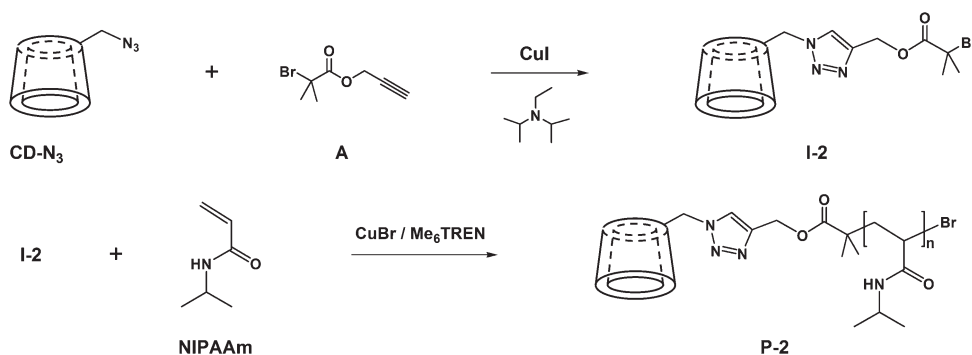


Figure 4. Reaction sequence for the synthesis of β -CD-PNIPAAm (**P-2**) via ATRP.

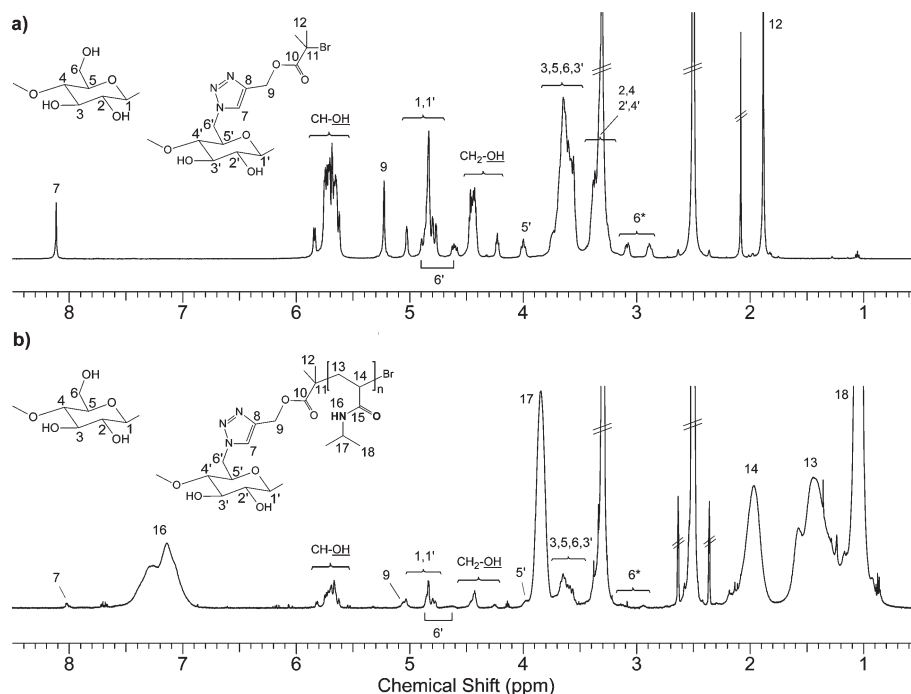


Figure 5. ¹H NMR spectra of initiator **I-2** (a) and polymer **P-2** (b) recorded in DMSO-*d*₆. Signals 6* are due to H₆ of the glucose unit bonded to C₁'.¹⁶

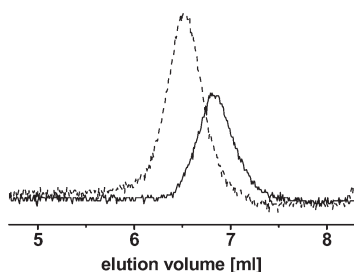


Figure 6. GPC chromatograms of **P-1** (solid line) and **P-2** (dashed line) obtained with LS-detector.

very well. This result together with the low PDI of **P-1** indicates a controlled polymerization process.

For **P-2**, the value determined by GPC via LS-detection ($M_{n,GPC} = 9600$ g/mol) and the one calculated from the ¹H NMR spectrum ($M_{n,NMR} = 9300$ g/mol) show a good agreement. However, considering the ratio [monomer]/[initiator], a lower

molar mass of polymer **P-2** was expected (4800 g/mol at a conversion of 100%). The observed deviation is probably due to a relatively low efficiency of initiator **I-2**. Additional ROESY experiment performed with the initiator **I-2** in a D₂O/DMF-*d*₇ mixture (1:1.9 v/v according to conditions of polymer synthesis) indicated that the methyl groups of the bromoisobutryl unit can be included in the CD ring. Thus, partial and dynamic dimer formation of **I-2** is in principle possible which can explain the low initiating efficiency. However, the narrow and symmetric molar mass distribution together with the low PDI of polymer **P-2** give rise to assume a controlled ATRP process. Thus, two water-soluble polymers, equipped with units for specific complexation (adamantane and β -CD, respectively) have been prepared.

Complexation Studies. To verify the interaction of β -CD- and adamantane-type polymer end groups in aqueous solution, complexation studies were carried out by ¹H NMR spectroscopy. Generally, NMR spectroscopy is the most important method to study the structure of host–guest interactions. Mainly the observations of chemical shift changes, the nuclear Overhauser

Table 1. Synthesis data and characteristics of P-1 and P-2

polymer	[monomer]/[initiator]	yield [%]	conversion [%]	$M_{n,th}$ [g/mol]	$M_{n,GPC}$ [g/mol]	$M_{n,NMR}$ [g/mol]	PDI ^e
P-1	50	58 ^a	92 ^c	4300 ^d	4600 ⁱ	4200 ^f	1.10
P-2	30	45 ^b	-	4800 ^g	9600 ^j	9300 ^h	1.10

^a Yield = $m_{polymer} / (m_{monomer} + m_{initiator} + n_{initiator}M_{capper} - n_{initiator}M_{HBr}) \times 100$, obtained after purification. ^b Yield = $m_{polymer} / (m_{monomer} + m_{initiator}) \times 100$, obtained after purification. ^c Monomer conversion: determined via NMR. ^d $M_{n,th} = conversion/100[monomer]/[initiator]M_{monomer} + M_{initiator} + M_{capper} - M_{HBr}$. ^e Determined via GPC (Light scattering (LS)-detector, solvent: DMAc + 3 g/L LiCl). ^f Calculated via NMR: integration of CH₃ signal of the repeating units vs aromatic protons signal of the initiating moiety, estimated relative error: $\pm 5\%$. ^g $M_{n,th} = [monomer]/[initiator]M_{monomer} + M_{initiator}$. (For this sample, $M_{n,th}$ was calculated for 100% conversion; the actual monomer conversion could not be determined). ^h Calculated via NMR: integration of CH₃ and CH₂ signal of the repeating units (0.7–1.8 ppm) vs. proton signals 1, 1', 6' and 9 (4.55–5.2 ppm) of the CD-moiety, estimated relative error: $\pm 5\%$. ⁱ $dn/dc = -0.104$ mL/g. ^j $dn/dc = -0.105$ mL/g.

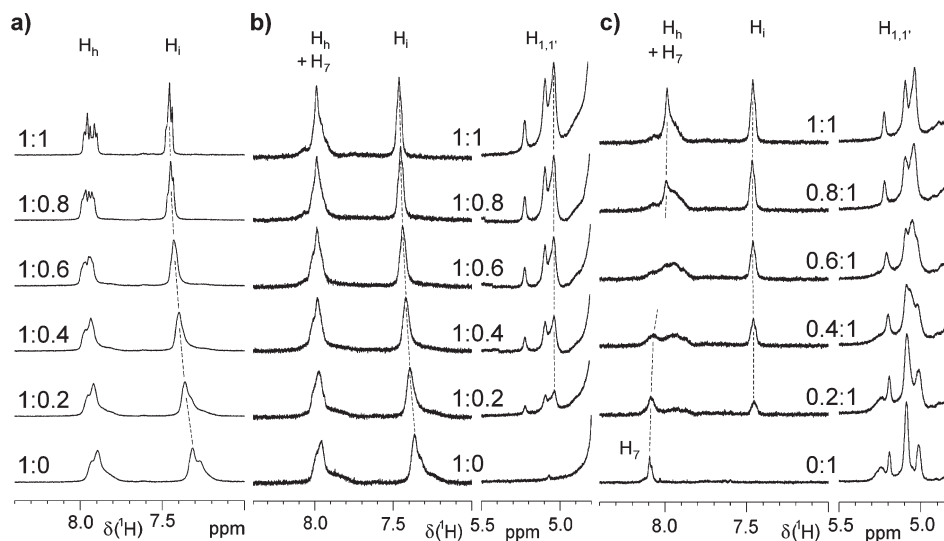


Figure 7. Regions from ¹H NMR spectra obtained for different ratios of (a) P-1 and successively added β -CD, (b) P-1 and successively added P-2, and (c) P-2 and successively added P-1 (D₂O, 30 °C). The molar ratios of Ada and β -CD moiety are given. The final concentration of both moieties was 5×10^{-3} M.

effects (nOes) but also of the diffusion behavior are major tools in structural studies of such complexes.^{33–35}

In a first step, the complexation of the adamantyl group of P-1 by β -CD was studied. Figure 7a depicts the signals of the benzoyl spacer between adamantane moiety and PMeOxa chain for different molar ratios of Ada-PMeOxa (P-1) and successively added β -CD. Changes in chemical shift and signal shape which were also observed for the signals of the adamantyl group itself prove an increasing content of complexed adamantyl end groups reaching almost complete complexation at 1:1 ratio in accordance with the large equilibrium constants of such complexes.²⁹ The significant narrowing of the signals of H_h and H_i in the course of titration is probably due to the different surrounding of the hydrophobic adamantane and benzoyl spacer moiety in D₂O and in the complex. The solvation should be poor in D₂O maybe resulting in ill-defined associates and interactions with the backbone whereas the well-defined surrounding in the β -CD cavity results in narrower lines as also observed in the good solvent DMSO-*d*₆ (Figure 3). The structure of the formed inclusion complex was studied by a ROESY spectrum (Figure 8). Intense correlation peaks between the aromatic protons and H₅ and H₆ of β -CD indicate that β -CD deeply includes the whole adamantyl end group together with the benzoyl spacer from the primary, i.e., the slightly narrower side of the β -CD ring. Accordingly, H_a and H_b of the adamantyl unit show correlation peaks with H₃ of β -CD and H_c with both H₃ and H₅ of β -CD. Such an insertion

mode was reported to be very stable for a structural similar β -CD/sodium 4-(1-adamantanyl)benzoate complex.³⁶

Parts b and c of Figure 7 represent regions from spectra obtained by titration of P-1 with P-2 (Figure 7b) and of P-2 with P-1 (Figure 7c), respectively. Whereas in the first case the changes in signal position and shape of the benzoyl protons indicate increasing content of complexed adamantane moieties, the increasing amount of β -CD rings covering adamantane moieties is indicated by changes in the H_{1,1'} and H₇ protons region of the β -CD end group. Other signals which could also be used to follow the complexation process, i.e., the adamantane protons and H₃ and H₅ of β -CD, are hidden by the large polymer signals. Finally, the same spectra were obtained at equimolar ratio of guest and host end group (top spectra in Figures 7b and 7c). Within the limits of the method, these findings prove formation of the desired inclusion complex with 1:1 stoichiometry. Unfortunately, a ROESY spectrum of this polymer complex gives no evaluable correlation peaks. Thus, the insertion mode could not be revealed directly. However, the changes observed for the benzoyl proton signals (Figure 7b) are similar to those observed for the complexation with free β -CD (Figure 7a). This suggests that also for polymer–polymer complexation the adamantyl end group is included in the β -CD cavity from the primary side. At first glance, this seems to be unlikely because the triazole ring, which connects the β -CD moiety with the PNIPAAm chain, is also located on this side. However, its flexibility is considered to

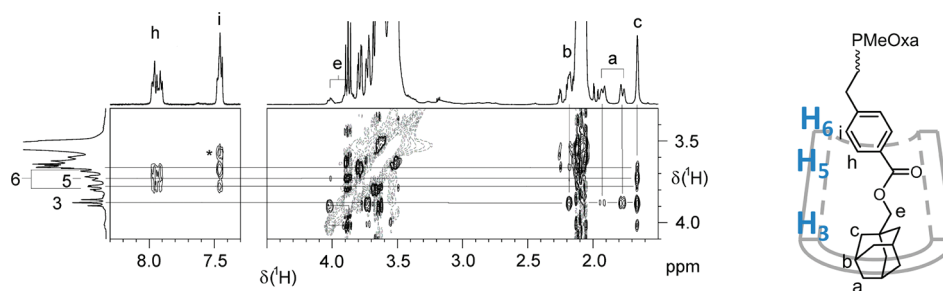


Figure 8. 2D ROESY spectrum of a 1:1 molar mixture of **P-1** and β -CD (both 5×10^{-3} M) in D_2O at $30^\circ C$ (mixing time $\tau_m = 248$ ms) and schematic representation of the detected insertion mode in the host–guest complex between the adamantane containing end group of **P-1** and β -CD.

be sufficiently high to allow for insertion of the adamantane moiety. Nevertheless, a direct prove of this insertion mode cannot be presented and thus, also adamantane insertion from the secondary side could occur or an equilibrium of both modes. Harada et al. reported such multimodes for the β -CD complexation with the adamantyl moieties of poly(4-(1-adamantyl)phenyl vinyl ether-*co*-sodium maleate).³⁶

Furthermore, dynamic light scattering (DLS) was tried to verify the complexation of **P-1** and **P-2**. The interaction between β -CD and adamantane is known to be particularly strong in water. However, DLS measurements in water turned out to be not conclusive due to additional strong intermolecular interactions and hence the formation of unspecific aggregates of varying particle sizes was observed. Therefore, further DLS measurements were done in dimethylacetamide (DMAc) in which the formation of unspecific aggregates is minimized and hence the particle sizes should be determined properly. However, in DMAc the binding constants for the Ada-CD complex are significantly smaller, and thus, it was only possible to determine the average size of the starting polymers **P1** (4 nm) and **P-2** (6 nm) but no efficient block copolymer formation could be confirmed by this methods (see Supporting Information). Similarly, GPC measurements on the self-assembled block copolymer showed the same limitations: strong aggregate formation in water as it was expected for that type of double-hydrophilic block copolymer and different complexation behavior in DMAc. The complex solution and aggregation behavior of the *sa P-1/P-2* block copolymers thus has to be the subject of a forthcoming more detailed study.

Thermoresponsive Behavior. With the self-assembled PNIPAAm–PMeOxa diblock copolymer in hand, the concept of heat-induced hydrophilic–hydrophobic switching of the PNIPAAm block in aqueous solution was studied with respect to the stability of the adamantane/ β -CD inclusion complex. First, such diblock copolymer was prepared by defined mixing of the polymers in D_2O under NMR observation (as described above) until complete complexation of the adamantane moiety by the β -CD unit was detected. Then the solvent was evaporated before redissolving the diblock complex for further analysis. The lower critical solution temperature (LCST) of the initial β -CD-PNIPAAm (**P-2**) and the yielded self-assembled complex (*sa P-1/P-2*) was determined by turbidimetry measurements using UV–vis spectrophotometry. Figure 9a shows the transmittance vs temperature plots (cloud point curves) for **P-2** and *sa P-1/P-2*. Both polymers show distinct heat-induced phase transitions with 50% transmittance points at about 37 and 41.5 $^\circ C$, respectively, with a significant broadening for *sa P-1/P-2*. Generally, the LCST of PNIPAAm can be influenced by several factors, e.g.

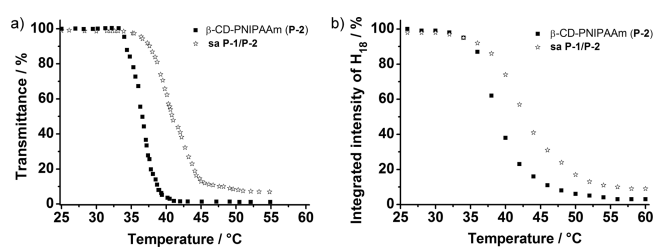


Figure 9. Transmittance (a) and integrated NMR intensity of the H_{18} signal (b) as a function of temperature for an aqueous solution of **P-2** and of the complex *sa P-1/P-2*, respectively (turbidimetry, 2 mg/mL solution in H_2O ; 1H NMR, 5×10^{-3} M solution in D_2O).

molecular weight, polydispersity and end groups, making the interpretation of such small effects problematic.^{37–39} Compared to the literature value of $32^\circ C$ reported for high-molecular-weight linear PNIPAAm,³⁸ the increased LCST of **P-2** can be attributed to both the rather low molecular weight ($M_{n,NMR} = 9300$ g/mol) and to the hydrophilic end group. The effect of complexation with **P-1** toward block copolymer structure on the LCST is moderate but obvious. Thus, extending the hydrophilic part by complexation with the water-soluble PMeOxa further increases the LCST by 4.5 K and leads to a less sharp transition. The increase in LCST is consistent with the behavior observed by Trellenkamp et al. with a different polymer system. In that study, a linear correlation was found between the adjusted hydrophilicity and the corresponding LCST of copolymers composed of *N*-vinyl-2-pyrrolidone and 3-ethyl-1-vinyl-2-pyrrolidone.⁴⁰

Several 1H NMR techniques provide a deeper insight into the behavior of structural units during such phase transitions, i.e., allow for following the temperature-induced processes on molecular level.⁴¹ Thus, we employed 1H NMR spectroscopy to study the temperature effect on both the spectrum of β -CD-PNIPAAm and of the block copolymer complex. The coil–globule phase transition at the LCST is accompanied by a virtual disappearance of signals. This is due to the fact that at temperatures above the LCST the mobility of most PNIPAAm units is reduced to such an extent that the lines become too broad to be detected in solution-state spectra. Thus, the integrated signal intensities can be used to characterize the phase transition behavior quantitatively. Figure 9b depicts the temperature dependence for the PNIPAAm methyl group signal obtained for **P-2** and the complex *sa P-1/P-2*. The intensity decrease with phase transition is less steep than observed in the turbidity measurements but the LCSTs correspond well: **P-2** 37 $^\circ C$ (turb.) vs 38.5 $^\circ C$ (NMR) and *sa P-1/P-2*: 41.5 vs 43 $^\circ C$. Thus, both methods show the same trend in increase in LCST upon block copolymer formation

and the small differences in the absolute LCST values determined by the two methods can be explained by the different block copolymers concentration used for the measurements. Again, the increase in LCST temperature due to complex formation is significant and is attributed to a “softening” effect on the PNIPAAm globules by the extended hydrophilic part in the self-assembled diblock and maybe also due to partial incorporation of PMeOxa in the outer sphere of the globules.

DSC measurements proved that both blocks are fully miscible (Figure 10) with a single transition temperature (T_g) of 92 °C for sa P-1/P-2 (P-1: 79 °C; P-2: 120 °C). Such a “softening” effect is the most probable explanation for the slightly higher content of still mobile component detected at the same temperature for sa P-1/P-2 compared with P-2.

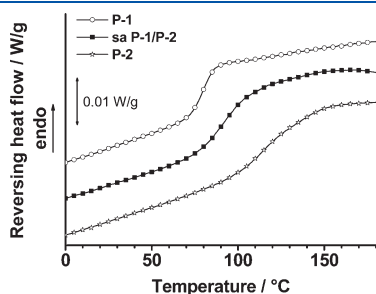


Figure 10. DSC curves (2nd heating cycle) of P-1 (cycles), P-2 (stars) and sa P-1/P-2 (squares).

Figure 11 shows a series of ^1H NMR spectra obtained for sa P-1/P-2 at different temperatures. The previously discussed loss of PNIPAAm signal intensity due to restricted mobility in the collapsed globular structures is obvious. The question arises whether the diblock copolymer complex still exists at higher temperatures or a separation in PNIPAAm globules and free moving PMeOxa coils occurs. If one compares the spectrum of sa P-1/P-2 (top spectrum of Figure 11b) and the corresponding spectrum of P-1 (Figure 11a), both recorded at 70 °C, the differences in signal position and shape are obvious for the aromatic and adamantyl protons of the Ada moiety. This suggests that PMeOxa is not released from the complex to a great extent. This is also in accordance with the almost unchanged signal position for the signals of H_h and H_i over the whole temperature region studied. The only change is in signal intensity and signal shape. The first effect is attributed to partial incorporation of connecting complexed PMeOxa block in the outer sphere of the collapsed PNIPAAm globules thus also resulting in reduced mobility and virtual signal loss. Only the still mobile chain components of the diblock complexes were detected. Surprisingly, the signal shapes at about the LCST become very similar to those observed for $\beta\text{-CD}/\text{P-1}$ complexes (Figure 7a), which was assigned by ROESY to the more stable insertion mode of Ada moiety from the primary side. This suggests that below LCST the complex in sa P-1/P-2 exists in different modes but at higher temperatures the most stable one with insertion from the primary side strongly dominates. The signal pattern of the PMeOxa backbone signals change slightly, i.e. see signal group of H_n in Figure 11b, but there is no loss of intensity. Furthermore, the

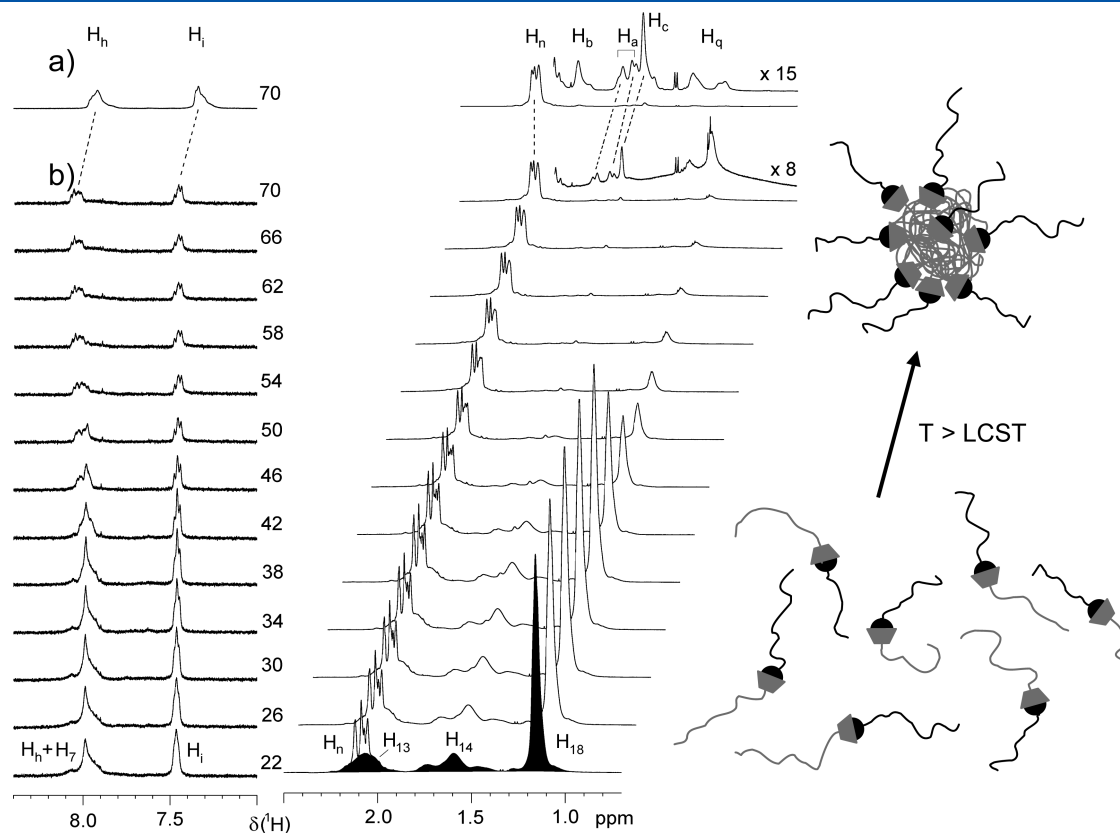


Figure 11. Regions from (a) the ^1H NMR spectrum of P-1 (5×10^{-3} M in D_2O) at 70 °C and (b) ^1H NMR spectra measured at different temperatures on a 5×10^{-3} M solution of sa P-1/P-2 (1:1 complex) in D_2O .

backbone signals are identical for **P-1** and **sa P-1/P-2** at, e.g., 70 °C (Figure 11a and top trace of Figure 11b) proving that this effect is not related to complex formation but to conformational changes of PMeOxa. Conclusively, at temperatures above LCST a globular core of collapsed PNIPAAm chains is surrounded by PMeOxa chains tethered by the β -CD/Ada complex formed from the corresponding polymer end group functionalities (scheme in Figure 11). This structure is similar to that of PNIPAAm-graft-PAlkylOxa copolymers reported in previous studies.^{31,42}

CONCLUSIONS

In this contribution, we described the combination of two water-soluble polymers to a defined thermoresponsive diblock copolymer through the noncovalent interaction of β -CD and adamantane. For that we developed a new synthetic strategy for the preparation of an adamantane end-functionalized poly(2-methyl-2-oxazoline) and a β -CD end-functionalized poly(*N*-isopropyl-acrylamide). The approach presented here includes the controlled polymerization of NIPAAm and 2-methyl-2-oxazoline with initiators that are functionalized with functional moieties able to form strong inclusion complexes. In this way, well-defined polymers were obtained, which undergo self-assembly to form the supramolecular diblock structure poly(2-methyl-2-oxazoline-*block-N*-isopropylacrylamide). The self-organized block formation could be verified undoubtedly by means of detailed NMR analysis.

Thus, we demonstrated for the first time the preparation of a well-defined diblock copolymer formed through self-assembly of cyclodextrin and adamantyl end-functionalized polymers. The described diblock assembly represents a double-hydrophilic system that is switchable to a hydrophilic–hydrophobic configuration by adjusting temperature. As detected by NMR spectroscopy, this thermal process leads to reversible polymer aggregation where a globular core of collapsed PNIPAAm chains is surrounded by PMeOxa chains, thus, representing a second self-assembly process which is thermally switchable. Therefore, this strategy leads to new reversibly thermoresponsive noncovalent diblock copolymers which can be fine-tuned in their aggregation behavior with potential use as drug delivery system.

ASSOCIATED CONTENT

S Supporting Information. Synthetic procedure of the alkyne 2-bromoisobutyl propargylester and the monoazide β -CD, mass spectrometry results (EI-MS) of the adamantyl functionalized initiator (**I-1**), experimental details and results of the MALDI-TOF analysis of Ada-PMeOxa (**P-1**), proton NMR results in DMSO of initiator **I-1** and of polymer **P-1** and the DLS diagrams of **P-1**, **P-2**, and **sa P-1/P-2** in DMAc are provided. This material is available free of charge via the Internet at <http://pubs.acs.org>.

AUTHOR INFORMATION

Corresponding Author

*E-mail: voit@ipfdd.de.

ACKNOWLEDGMENT

The authors thank Mr. Andreas Korwitz for assistance in NMR measurements, Dr. Alben Lederer and Ms. Petra Treppe for GPC measurements, and Ms. Liane Häussler for DSC

analysis. Dr. Karin Sahre is thanked for MALDI studies. We would further like to thank Dr. Maricica Munteanu for synthesis of mono(6-azido-6-desoxy)- β -cyclodextrin.

REFERENCES

- (1) Kollisch, H. S.; Barner-Kowollik, C.; Ritter, H. *Chem. Commun.* **2009**, 1097–1099.
- (2) Cesteros, L. C.; Gonzalez-Teresa, R.; Katime, I. *Eur. Polym. J.* **2009**, *45*, 674–679.
- (3) Nozaki, T.; Maeda, Y.; Kitano, H. *J. Polym. Sci., Polym. Chem.* **1997**, *35*, 1535–1541.
- (4) van de Manakker, F.; Vermonden, T.; van Nostrum, C. F.; Hennink, W. E. *Biomacromolecules* **2009**, *10*, 3157–3175.
- (5) Li, J.; Loh, X. J. *Adv. Drug Delivery Rev.* **2008**, *60*, 1000–1017.
- (6) Li, J. S.; Xiao, H. N.; Li, J. H.; Zhong, Y. P. *Int. J. Pharm.* **2004**, *278*, 329–342.
- (7) Xin, J. Y.; Guo, Z. Z.; Chen, X. Y.; Jiang, W. F.; Li, J. S.; Li, M. L. *Int. J. Pharm.* **2010**, *386*, 221–228.
- (8) Li, L.; Guo, X. H.; Wang, J.; Liu, P.; Prud'homme, R. K.; May, B. L.; Lincoln, S. F. *Macromolecules* **2008**, *41*, 8677–8681.
- (9) Kretschmann, O.; Choi, S. W.; Miyauchi, M.; Tomatsu, I.; Harada, A.; Ritter, H. *Angew. Chem., Int. Ed.* **2006**, *45*, 4361–4365.
- (10) Kretschmann, O.; Steffens, C.; Ritter, H. *Angew. Chem., Int. Ed.* **2007**, *46*, 2708–2711.
- (11) Charlot, A.; Auzely-Velty, R. *Macromolecules* **2007**, *40*, 9555–9563.
- (12) Guerrouache, M.; Millot, M. C.; Carbonnier, B. *Macromol. Rapid Commun.* **2009**, *30*, 109–113.
- (13) Gonzalez-Campo, A.; Hsu, S. H.; Puig, L.; Huskens, J.; Reinhoudt, D. N.; Velders, A. H. *J. Am. Chem. Soc.* **2010**, *132*, 11434–11436.
- (14) Choi, S.; Munteanu, M.; Ritter, H. *J. Polym. Res.* **2009**, *16*, 389–394.
- (15) Trellenkamp, T.; Ritter, H. *Macromolecules* **2010**, *43*, 5538–5543.
- (16) Nielsen, T. T.; Wintgens, V.; Amiel, C.; Wimmer, R.; Larsen, K. L. *Biomacromolecules* **2010**, *11*, 1710–1715.
- (17) Lehn, J. M. *Polym. Int.* **2002**, *51*, 825–839.
- (18) De Greef, T. F. A.; Smulders, M. M. J.; Wolfs, M.; Schenning, A.; Sijbesma, R. P.; Meijer, E. W. *Chem. Rev.* **2009**, *109*, 5687–5754.
- (19) Cordier, P.; Tournilhac, F.; Soulie-Ziakovic, C.; Leibler, L. *Nature* **2008**, *451*, 977–980.
- (20) Folmer, B. J. B.; Sijbesma, R. P.; Versteegen, R. M.; van der Rijt, J. A. J.; Meijer, E. W. *Adv. Mater.* **2000**, *12*, 874–878.
- (21) Feldman, K. E.; Kade, M. J.; Meijer, E. W.; Hawker, C. J.; Kramer, E. J. *Macromolecules* **2010**, *43*, 5121–5127.
- (22) Tang, C. B.; Lennon, E. M.; Fredrickson, G. H.; Kramer, E. J.; Hawker, C. J. *Science* **2008**, *322*, 429–432.
- (23) Ott, C.; Kranenburg, J. M.; Guerrero-Sanchez, C.; Hoepfener, S.; Wouters, D.; Schubert, U. S. *Macromolecules* **2009**, *42*, 2177–2183.
- (24) Chiper, M.; Meier, M. A. R.; Wouters, D.; Hoepfener, S.; Fustin, C. A.; Gohy, J. F.; Schubert, U. S. *Macromolecules* **2008**, *41*, 2771–2777.
- (25) Chiper, M.; Fournier, D.; Hoogenboom, R.; Schubert, U. S. *Macromol. Rapid Commun.* **2008**, *29*, 1640–1647.
- (26) Ozyurek, Z.; Voit, B.; Krahl, F.; Arndt, K. F. *e-Polym.* **2010**, *13*.
- (27) Chang, C.; Wei, H.; Quan, C. Y.; Li, Y. Y.; Liu, J.; Wang, Z. C.; Cheng, S. X.; Zhang, X. Z.; Zhuo, R. X. *J. Polym. Sci., Polym. Chem.* **2008**, *46*, 3048–3057.
- (28) Wei, H.; Zhang, X. Z.; Cheng, C.; Cheng, S. X.; Zhuo, R. X. *Biomaterials* **2007**, *28*, 99–107.
- (29) Rekharsky, M. V.; Inoue, Y. *Chem. Rev.* **1998**, *98*, 1875–1917.
- (30) David, G.; Alupei, V.; Simionescu, B. C.; Dincer, S.; Piskin, E. *Eur. Polym. J.* **2003**, *39*, 1209–1213.
- (31) Rueda, J.; Zschoche, S.; Komber, H.; Schmaljohann, D.; Voit, B. *Macromolecules* **2005**, *38*, 7330–7336.

- (32) Gawronski, J. K.; Reddy, S. M.; Walborsky, H. M. *J. Am. Chem. Soc.* **1987**, *109*, 6726–6730.
- (33) Schneider, H. J.; Hacket, F.; Rudiger, V.; Ikeda, H. *Chem. Rev.* **1998**, *98*, 1755–1785.
- (34) Wenz, G.; Han, B. H.; Muller, A. *Chem. Rev.* **2006**, *106*, 782–817.
- (35) Cohen, Y.; Avram, L.; Frish, L. *Angew. Chem., Int. Ed.* **2005**, *44*, 520–554.
- (36) Taura, D.; Taniguchi, Y.; Hashidzume, A.; Harada, A. *Macromol. Rapid Commun.* **2009**, *30*, 1741–1744.
- (37) Plummer, R.; Hill, D. J. T.; Whittaker, A. K. *Macromolecules* **2006**, *39*, 8379–8388.
- (38) Schild, H. G. *Prog. Polym. Sci.* **1992**, *17*, 163–249.
- (39) Xia, Y.; Burke, N. A. D.; Stover, H. D. H. *Macromolecules* **2006**, *39*, 2275–2283.
- (40) Trellenkamp, T.; Ritter, H. *Macromol. Rapid Commun.* **2009**, *30*, 1736–1740.
- (41) Spevacek, J. *Curr. Opin. Colloid Interface Sci.* **2009**, *14*, 184–191.
- (42) Rueda, J. C.; Zschoche, S.; Komber, H.; Krahl, F.; Arndt, K. F.; Voit, B. *Macromol. Chem. Phys.* **2010**, *211*, 706–716.